

ORIGINAL ARTICLE

Special Section: Tribute to Rien van Genuchten, Recipient of the 2023 Wolf Prize for Agriculture

Multiscale pore-network reconstruction of a fine-textured heterogeneous soil

Elizabeth M. Pontedeiro^{1,2}  | Martinus Th. van Genuchten^{1,3}  | William Godoy²  |
 Mateus G. Ramirez⁴  | Carlos M. P. Vaz⁵  | Silvio Crestana⁵ | Maira C. O. Lima² |
 Paulo Couto²  | Jian Su³

¹Department of Earth Sciences, Utrecht University, Utrecht, The Netherlands

²Department of Civil Engineering, Federal University of Rio de Janeiro, Rio de Janeiro, Rio de Janeiro, Brazil

³Department of Nuclear Engineering, Federal University of Rio de Janeiro, Rio de Janeiro, Rio de Janeiro, Brazil

⁴Department of Mechanical Engineering, Federal University of Rio de Janeiro, Rio de Janeiro, Rio de Janeiro, Brazil

⁵Embrapa Agricultural Instrumentation, São Carlos, São Paulo, Brazil

Correspondence

Elizabeth M. Pontedeiro, Department of Earth Sciences, Utrecht University, Princetonlaan 8a, 3584 CB, Utrecht, The Netherlands. Email:

bettinadulley@hotmail.com

Assigned to Associate Editor Jirka Simunek.

Abstract

Digital samples offer many opportunities to study subsurface fluid flow and contaminant transport processes. The pore size distribution of especially fine-textured porous media often covers many orders of magnitude in the length scale, which makes accurate microCT scanning and modeling of the underlying processes difficult. When a single-resolution image is not capable of capturing all relevant details of a sample, one should scan the sample, or selected parts of it, at different resolutions. Combining multiple resolutions into one single sample for subsequent pore-scale modeling is generally not possible due to limitations in computer memory and speed, thus making it necessary to create a simpler sample containing relevant information from the parent networks. We imaged four samples using different resolutions to capture the multiscale heterogeneity of a fine-textured soil and combined them into one overall digital sample based on the original pore networks. The parent networks were characterized using their geometrical properties, correlations between these properties, and connectivity functions describing the network topologies. Our approach creates stochastic networks of arbitrary size with the same flow properties as the parent network. The method, implemented using the PoreStudio pore network model, repeatedly integrates information at two subsequent scales, with the resulting digital sample having the same hydraulic properties as the original samples. The procedure leads to more useful three-dimensional digital models, facilitating basic analyses of underlying pore size distributions. Porosity calculations were compared with direct measurements, while those for the hydraulic conductivity were compared with estimates based on the particle size distribution and nearby field data.

Abbreviations: μ CT, computed microtomography; CV, coefficient of variation; DPA, digital pore analysis; PNM, pore network model; PSD, pore size distribution; REV, representative elementary volume.

This is an open access article under the terms of the [Creative Commons Attribution](https://creativecommons.org/licenses/by/4.0/) License, which permits use, distribution and reproduction in any medium, provided the original work is properly cited.

© 2024 The Author(s). *Vadose Zone Journal* published by Wiley Periodicals LLC on behalf of Soil Science Society of America.

1 | INTRODUCTION

A major motivation of pore-scale imaging using X-ray computed microtomography (μ CT) is to estimate properties of porous media using nondestructive methods. Improvements in high-resolution digital imaging and computerized image analysis now enable one to characterize the microstructure of a range of natural and engineered porous materials, including soils and rocks (e.g., Allaire et al., 2009; Cnudde & Boone, 2013; Godoy et al., 2019; Katuwal et al., 2018; Lima et al., 2020; Salek & Beckingham, 2023; Vaz et al., 2014; Wildenschild & Sheppard, 2013).

MicroCT has become popular since it provides three-dimensional (3D) volumetric imaging data of undisturbed samples. Pore-scale characterization of porous media is important for many practical applications involving multiphase fluid flow and the transport of a range of agricultural and industrial contaminants. Flow and transport processes in such applications are closely related to pore size, pore shape, and the connectivity between pores. X-ray μ CT provides an excellent non-invasive means for characterizing dynamic pore-scale processes (e.g., Van Offenwert et al., 2019). The digital reconstruction of image stacks permits representations of the internal pore structure of a sample, the connection of pores within the pore network, and the underlying flow and transport processes. Many different approaches can be used to model pore-scale processes, such as various lattice Boltzmann formulations, coupled computational fluid dynamics-discrete element methods (Elrahmani et al., 2022), and pore network models (PNMs) (Raoof et al., 2013). For our studies, we used a PNM because it is computationally less demanding than direct methods and permits one to incorporate more heterogeneity when modeling larger volumes.

Porosity and permeability are key porous media parameters affecting fluid flow and contaminant transport processes. Porosity can be estimated from 3D imaging data by converting grayscale images into binary ones representing solid material and void spaces. Many previous studies indicate that a more complete characterization of the pore size distribution (PSD) of μ CT images requires the estimation of pore sizes taken from multi-resolution images, and then combining the information from each resolution to obtain the complete PSD (Cássaro et al., 2017; Jiang et al., 2007; Vaz et al., 2011; Yang et al., 2009). Thus, the first step of our work was to evaluate images of soils generated using μ CT and, according to the property being studied, to define if possible an optimal imaging resolution for comparison with the measurements.

Soils and rocks generally consist of a range of micro- and macropores, which together define the overall connected pore structure of the medium. The differently sized pores are known to contribute to distinct yet interacting water flow and contaminant transport processes. In saturated media, the larger pores will favor overall fluid flow processes (including

Core Ideas

- A stochastic method was used to combine four computed microtomography samples with different resolutions into one digital sample.
- The approach was applied to a fine-textured tropical soil with a very broad pore-size distribution.
- The methodology kept the same digital porosity as the original pore networks and enhanced the flow properties.

preferential flow) and contribute the most to the permeability of the sample, while the smaller pores are important for capillarity, fluid retention, diffusion, and chemical reaction processes. Recent advances in CT facilitate the acquisition of high-resolution images of 3D porous media, thus permitting more precise studies about the double- or triple-porosity characteristics of macro-porous soils and fractured rock (Jiang et al., 2013; Katuwal et al., 2018; Ruspini et al., 2021; Sadeghnejad & Gostick, 2020; Wildenschild & Sheppard, 2013; among others).

A major limitation of image-based soil and rock porosity measurements derived solely from μ CT data is that pores smaller than the voxel size cannot be detected (Cássaro et al., 2017; Jiang et al., 2012; Pak et al., 2016). Using existing μ CT instrumentation to properly characterize heterogeneous samples having PSDs spanning several orders of magnitude is especially challenging since the evaluated “digital” porosity/permeability is generally smaller than measured in the laboratory. The resulting underestimation of porosity can lead to errors in the water retention and hydraulic conductivity/permeability calculations, and hence fluid flow and contaminant transport processes in porous media. To compensate for this, advanced image processing techniques must be used for soils and rocks to account for their possible dual porosity properties. For dual- or triple-porosity media, which includes many tropical soils (e.g., oxisols and latosols) and carbonate rocks, new imaging and modeling techniques have been introduced to capture the full range of the pore structure features. These include approaches using machine learning (Dragonfly, 2022) or cellular automata and micro-computed tomography (Zubeldia et al., 2016), among others. The simulation and modeling of physical parameters using non-destructive techniques such as high-resolution tomography opens new opportunities for dynamic studies at different scales, like synchrotron-based tomography (Menke et al., 2016), including the dynamics of unsaturated flow in soils. One challenge is the integration and interpretation of results at different scales (downscaling and upscaling), such as from the use of different types of μ CTs (Crestana & Cruvinel, 2023).

MicroCT imaging techniques suffer from limitations in terms of a trade-off between resolution and sample size. In practice, the images that are obtained via μ CT may be unable to capture all aspects of the pore system of any realistic medium. The issue is twofold: some porous media contain noticeable fractions of micro-porosity that cannot be resolved at micron-scale resolutions, while using a sub-micron resolution implies that the resulting sample volume is too small to capture the heterogeneity of the macro-porosity. One approach is to combine images taken at different resolutions into one global image (Hebert et al., 2014; Jiang et al., 2012; Kastner et al., 2021; Vaz et al., 2014; Wu et al., 2011; Yao et al., 2023). For example, Jiang et al. (2012) developed a stochastic approach to combine the observed networks at different resolutions into a simpler overall network with very similar overall properties.

While pore network modeling is considered to be an important tool for simulating complex physical processes at the pore scale, Pore network model (PNM) predictions often do not agree well with the corresponding laboratory measurements, especially when complex pore systems are present (Pak et al., 2016). PNMs simplify the geometry of the pore space and generally cannot capture all of the characteristics of porous media due to a lack of resolution. The trade-off between sample size and μ CT image resolution means that a single μ CT volume may not capture all details of a multiscale pore structure. The realism and precision of the modeling results depends on the constructed global pore network assumed to be its complete representation (Xiong et al., 2016), as well as whether the overall sample can be considered a representative elementary volume (REV) of its physical properties.

The REV is defined as the minimum volume of a certain property that is large enough to capture a representative amount of heterogeneity, or the minimum volume in which the property is insensitive to small changes in volume or sample location. Location here means that the REV is the largest quantity insensitive to small changes in volume throughout the entire medium. The REV may vary for different properties (Vik et al., 2013), with the porosity REV usually being smaller than the permeability REV because of macroscopic variability in the latter. Selecting a region with proper REV characteristics is as important as the invoked mathematical model to obtain good results with adequate computational cost (Blunt et al., 2013; Mehmani et al., 2020; Piccoli et al., 2019; Verri et al., 2017). Since fluid flow only occurs in the connected porosity, 50% of the flow process in many soils and rocks may well occur in only 10% of the pores (e.g., Mehmani et al., 2020).

Main objective of this paper is to use images at different resolutions to provide global estimates of porosity and permeability, and the resulting fluid flow process. Digital soil samples were generated using μ CT images and the main characteristics of the imaged soil (the skeleton components),

and then compared to those of the original sample. Multi-scale imaging and pore-scale modeling, along with statistical functions based on the original pore networks, were used to obtain the new digital soil sample. The resulting 3D networks hence were combined and transformed into one multiscale pore network. For this, we used the skeleton of the lower resolution (sample BS4) and added the micro- and meso-porosity characteristic (pore throats and pore bodies) from the higher resolution samples such that the multiscale pore system of the digital sample honored the average connectivity of the sample. The digital soil sample was generated numerically using the pore-scale network model within the PoreStudio software (PoreStudio, 2023), an update of the PoreFlow software of Raouf et al. (2013).

2 | EXPERIMENTAL

This section describes the measurements, μ CT acquisition, the numerical simulations, and other analyses that were carried out using the soil samples.

2.1 | Sample selection and soil physical properties

The μ CT and modeling studies were carried out using four samples taken from an undisturbed block of a Brazilian tropical oxisol (Rhodic Hapludox). Sample selection, their imaging with μ CT, and the laboratory measurements were carried out by Embrapa/CNPDIA. Complete descriptions of the soils and experimental procedures are provided by Vaz et al. (2011, 2014); they are briefly described below.

A cubic sample of undisturbed soil, 20 cm on each side, was collected at a depth of 20 cm below the surface at the Embrapa Southeast Cattle Experimental Farm in the city of São Carlos, Brazil. The sample was dried at room temperature for 30 days and then cut into two equal parts. One part was used for measurements of physical properties such as the soil particle density (using the pycnometer method), the bulk density, and the particle size distribution (data in Vaz et al. [2011, 2014] and Cássaro et al. [2017]), and the other part was used to obtain several samples in the form of cylinders of different sizes to perform the μ CT analyses with a series of resolutions. Mercury intrusion porosimetry was used to measure the total porosity ($0.502 \text{ cm}^3/\text{cm}^3$), while the bulk density was estimated to be $1.13 \text{ g}/\text{cm}^3$. The particle size distribution by weight was found to be 12% sand, 9% silt, and 79% clay. Embrapa/CNPDIA used four different sample sizes (cylinders) to obtain the soil μ CT images in four distinct resolutions. Sample sizes in terms of their diameter and height were $0.5 \times 0.5 \text{ cm}$ (sample BS1), $1.0 \times 2.0 \text{ cm}$ (sample BS2), $2.0 \times 2.0 \text{ cm}$ (sample BS3), and $4.0 \times 2.5 \text{ cm}$ (sample BS4). The samples



FIGURE 1 Four cylindrical undisturbed soil samples extracted from a soil block collected at 0–20 cm of a Brazilian oxisol (Rhodic Hapludox) with different diameters: 4 cm (BS4), 2 cm (BS3), 1 cm (BS2), and 0.5 cm (BS1).

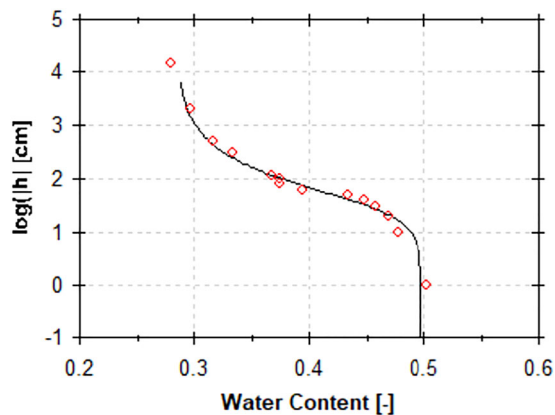


FIGURE 2 Observed (data) and fitted (solid line) water retention curves of the fine-textured soil.

were wrapped with parafilm to avoid losing soil particles during data acquisition, fixed onto the microtomography sample stage, and scanned with spatial resolutions (pixel sizes) of 3.6, 6, 12, and 25 μm for samples BS1, BS2, BS3, and BS4, respectively. Figure 1 shows pictures of the four samples.

Figure 2 shows the measured water retention curve of the soil, along with the fitted van Genuchten–Mualem function (van Genuchten, 1980). Fitted values of the saturated (θ_s) and residual (θ_r) water contents and the semi-empirical shape factors α and n were as follows: $\theta_s = 0.497 \text{ cm}^3/\text{cm}^3$, $\theta_r = 0.284 \text{ cm}^3/\text{cm}^3$, $\alpha = 0.028 \text{ 1/cm}$, and $n = 1.750$. Unfortunately, no direct data of the saturated hydraulic conductivity (K_s) were available of the soil block we used. We used the Rosetta pedo-transfer function software of Schaap et al. (2001) to obtain an approximate estimate of K_s from the particle size distribution and the bulk density. A 24.7 cm/day value was obtained, consistent with the average of several K_s measurements at field locations near the sampling site (Vaz et al., 2014).

2.2 | Multi-scale μCT measurements

Microtomography images were acquired with a cone beam benchtop X-ray microCT scanner from SkyScan, model 1172 (Bruker). The X-ray tube operated at 100 kV and 100 mA. The soil samples were rotated stepwise by 0.3° over 360° , while 15 frames were acquired and averaged to represent the shadow projection of each rotational step. The samples were wrapped with parafilm to avoid losing soil particles during data acquisition and fixed onto the μCT scanner stage with double-sided tape and modeling clay to avoid any movement of the samples during rotation (for more detail, see Cássaro et al. [2017]).

Each soil sample was scanned using four distinct resolutions to permit not only studies of the internal network of the pores but also to explore the effect of imaging resolution on the distribution of pore sizes and the equivalent pore diameters. The scans showed that sample BS1 had a very fine network, samples BS2 and BS3 had fine to intermediate networks, and sample BS4 had a coarse network. Table 1 shows the resolution, the porosity obtained from the μCT images, the connected porosity given by the skeleton, and the hydraulic conductivity obtained for each sample after modeling with the PoreStudio software using pore network modeling. Our modeling results showed that the connected porosity and the expected hydraulic conductivity obtained using Rosetta could not be reached using only one resolution of the μCT scans.

Cássaro et al. (2017) noted that the soil showed much variability in terms of its structure because of the presence of large, relatively dense aggregates of about 5 mm in diameter, possibly because of the intra-aggregate pores in this heavy clay soil. The soil total porosity could not be obtained directly from the μCT images since part of the fine-textured (clayey) medium contained many pores with diameters smaller than the best resolution of the scans (3.6 μm for sample BS1). The loss of part of the porosity (smaller pores or bigger pores) can impact directly on the modeling of the fluid flow and transport inside the sample, once the pores that are not part of the microCT pore network can break relevant connections among percolation clusters at the skeleton of the sample.

The μCT stacks were reconstructed and analyzed with the Avizo 2022.2 software (Thermo Fisher Scientific, 2022). We developed scripts in Mathematica 12.3 (2021) to track the diameters and 3D coordinate pore paths, and obtain input data for pore network modeling. The images of μCT , the porous media, and the skeleton given by Avizo 2022.2 were obtained using 501 slices/stack for the BS1/2/3 samples and 301 slices for the BS4 stack.

2.3 | Pore network modeling

Pore network modeling was carried out using the new PoreStudio software (Lima et al., 2022; PoreStudio, 2023),

TABLE 1 MicroCT porosity and saturated hydraulic conductivity values of the four samples.

Sample	μ CT resolution (μm)	μ CT porosity (cm^3/cm^3)	Connected porosity (cm^3/cm^3)	Hydraulic conductivity, K_s (cm/day)
BS1	3.6	0.240	0.110	36.1
BS2	6	0.207	0.127	22.41
BS3	12	0.121	0.071	17.34
BS4	25	0.043	0.014	10.98

which comprises a cross-platform pore network code and associated solver. The software allows simulations of a full range of flow and transport processes based on several modules. The different modules permit one to model single and multiphase flow, tracer transport in single and multiphase systems, and reactive contaminant transport in a single phase. The software can use the skeleton data extracted from μ CT images or generate a statistically equivalent network using geometrical parameters (e.g., pore size and pore throat radii) and morphological parameters (e.g., pore connectivity) based on analysis of the sample skeleton. Here, we give only a very short description of the PNM approach used in the PoreStudio software. We refer to Raouf and Hassanizadeh (2010) and PoreStudio (2023) for more details.

The PNM uses pore bodies (nodes) and pore throats with a specific topological configuration, with the pore throats prescribing the connections between pore bodies. The larger pore bodies are modeled as spheres, and the pore throats are modeled as capillary tubes to serve as connections between the pore bodies. During quasi-static single-phase flow, a pressure gradient is established in the pore network between the input and output boundaries of the PNM along the flow direction. Numerical simulations were carried out assuming connectivity between the top and bottom of the sample (the z -axis), being the direction of flow within the plugs. Volumetric flow through the pore throats is assumed to be laminar and described by the Hagen–Poiseuille equation:

$$Q_{ij} = g_{ij}(p_j - p_i) \quad (1)$$

where Q_{ij} is the volumetric flow rate through the pore throat between two adjacent pore bodies (i and j), p_i and p_j are the pressures at the two pore bodies, and g_{ij} is the conductance of the cylindrical shaped pore throat whose value can be obtained using:

$$g_{ij} = \frac{\pi R_{ij}^4}{8\mu l_{ij}} \quad (2)$$

in which R_{ij} is the radius of the pore throat, l_{ij} is the length of the throat, and μ is the dynamic viscosity of the fluid (water). Considering a well-defined volume sample, the average velocity of fluid in the pore, \bar{v} , is then (Raouf et al.,

2013):

$$\bar{v} = \frac{Q_{\text{tot}}L}{V_f} \quad (3)$$

where Q_{tot} is the total flow rate through the pore network, which can be determined at the inlet or outlet of the pore network as the sum of all flows, L is the length of the pore network, and V_f is the total volume of the liquid phase within the pore network. The absolute permeability K_s of the sample is then calculated using Darcy's equation. A small differential of pressure was adopted to guarantee laminar flow (low Reynolds number). The initial moisture condition is assumed to be full saturation.

In the present study, the software used the skeleton extracted directly from the μ CT images. The program initially gives the number of pore throats and pore bodies. Some results, such as porosity, permeability, and the average coordination number, are related to the connected pores (clusters). PNM modeling details are provided in Table 2, while Figure 3 shows the μ CT images and the sample porous media at four different resolutions.

A digital pore analysis (DPA) was further performed to analyze the distribution of several parameters inside the samples. The PNM approach assumes that the pore space is a network (the skeleton) with a simplified geometry represented by spherical pore bodies and connecting cylindrical pore throats. Despite being a simplified structure, the skeleton typically comprises thousands of points, requiring statistical techniques for quantitative assessments. A script was developed for the DPA (Silveira et al., 2022) to make it possible to evaluate the distribution of total porosity and of the pore-throat and pore-body porosities along the samples. The sample for this purpose was divided longitudinally into 20 sections. Figure 4 shows the observed skeletons and distributions of the three porosities along the 20 sections. The data indicate that the pore throat and pore body porosity distributions along samples BS1 and BS3 (3.6 and 12 μm) are very similar, while samples BS2 and BS4 show a more heterogeneous porosity distribution with higher pore throat porosities at sections 9 (BS2) and 10 (BS4), respectively.

The frequencies of the coordination number are shown in Figure 5 for all samples. Sample BS2 (6 μm) showed the best

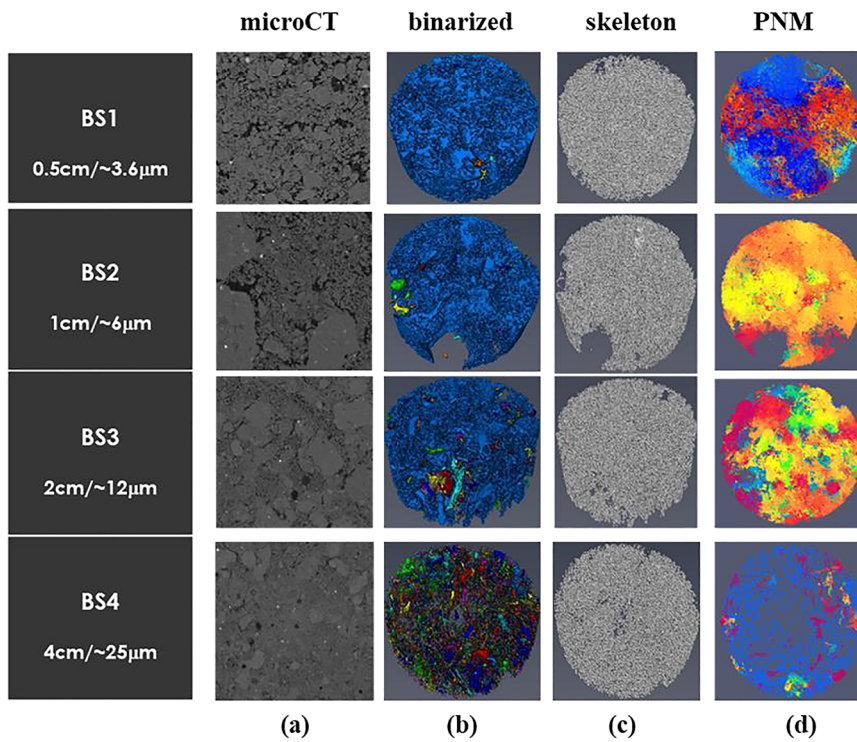


FIGURE 3 Images of the BS soil samples at different resolutions: (a) a micro slice, (b) the binarized image, (c) the skeleton image generated with Avizo, and (d) the pressure distribution inside the sample as calculated with the PoreStudio pore network model (PNM).

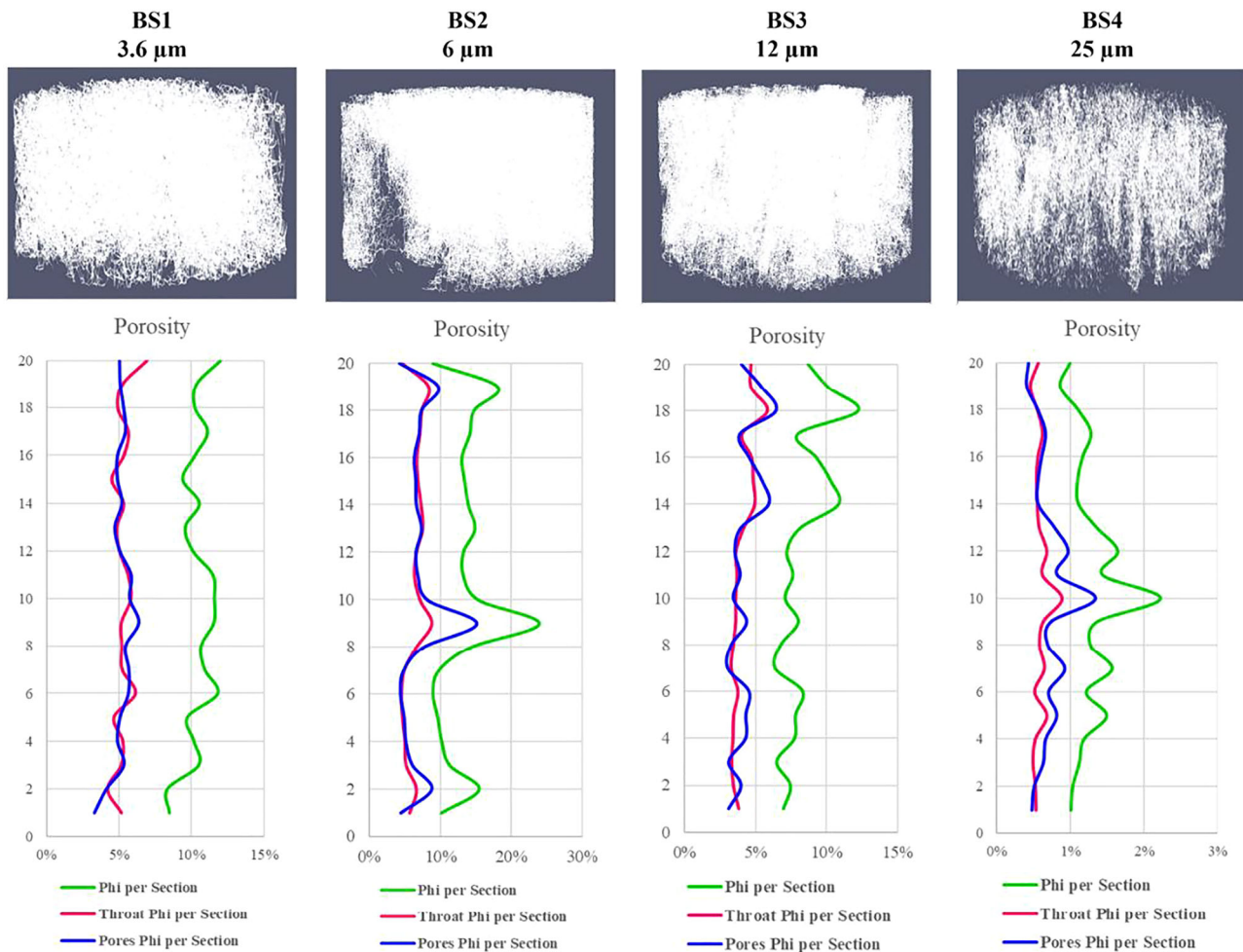


FIGURE 4 Longitudinal distributions of the different total, pore throat and pore body porosities (Phi) along the four soil samples.

TABLE 2 Pore network model (PNM) parameters of the four subsamples.

Sample	Pore throats	Pore bodies	Domain dimension (voxels)	Average coordination number
BS1	118,686	79,544	1300 × 1300 × 300	2.98
BS2	341,586	230,934	1600 × 1600 × 300	2.98
BS3	179,735	172,143	1700 × 1700 × 300	2.88
BS4	65,844	60,476	1550 × 1550 × 150	1.76

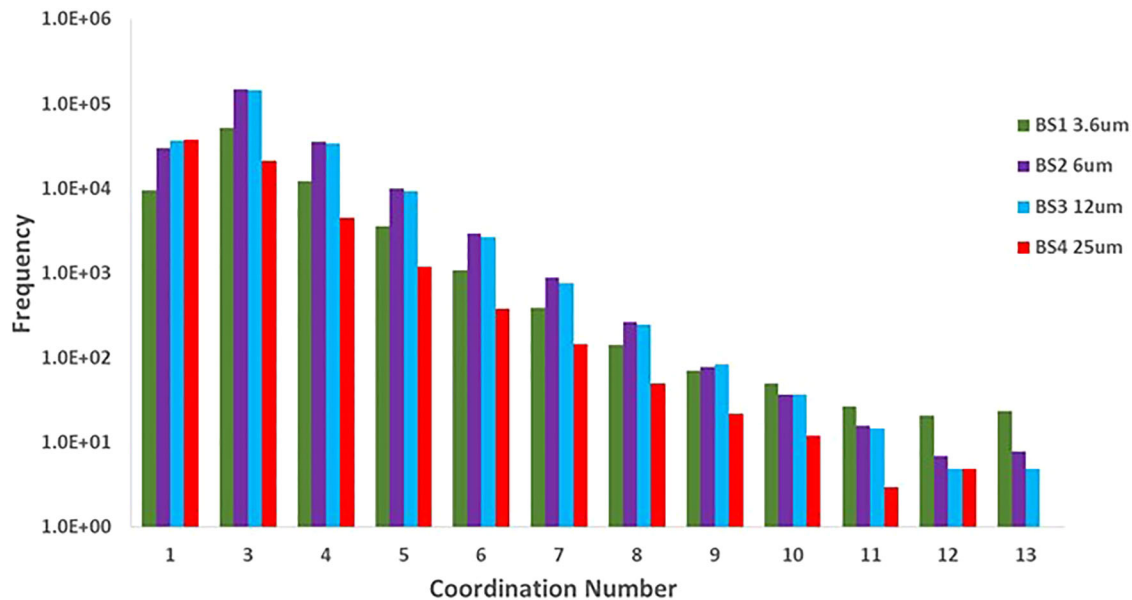


FIGURE 5 Coordination number versus frequency of the soil samples.

pore connectivity in the samples, followed by sample BS3 (25 μm).

We also calculated the distribution of pore throat and pore body volumes per radius in terms of voxels. Results in Figure 6 show that sample BS2 has the highest volumes for both the pore throats and pore bodies, followed by sample BS3. The DPA data explained that the samples with the best connectivity and higher volumes of pore throats and pore bodies present higher hydraulic conductivities when modeling using the PNM.

3 | MULTI-RESOLUTION ANALYSIS

In order to improve the modeling of a sample having different orders of magnitude in the size of their pores, we combined information of the samples with distinct spatial scales and μCT image resolutions into one overall global digital sample. For this, we used stochastic networks of arbitrary size with the same fluid flow properties as the initial or parent networks. This was done in four steps. First, we characterized the parent networks in terms of distributions of the geometrical pore

properties and correlations between these properties, as well as the connectivity function describing the detailed network topology. Second, to create a stochastic network of arbitrary size, we generated the required number of nodes and bonds with the correlated properties of the original network. The nodes were randomly located in the given network domain and connected by bonds according to the strongest correlation between node and bond properties, while honoring the connectivity function. Then, using the generated stochastic networks, we used PoreStudio to integrate two networks created in the same domain into a single two-scale network by characterizing the cross-scale connection structure between the two networks. Finally, multiscale networks were generated by repeating the above scheme. The overlap/combination of the networks ensured a better representation of the overall pore network.

To apply the described method, a REV is required. We used two samples of our set (BS2 and BS4) to verify if they represented reasonable REV. This choice was based on the fact that BS2 gave a hydraulic conductivity closer to the one estimated, while BS4 had the larger network to which those of the finer resolutions could be added. The combination of

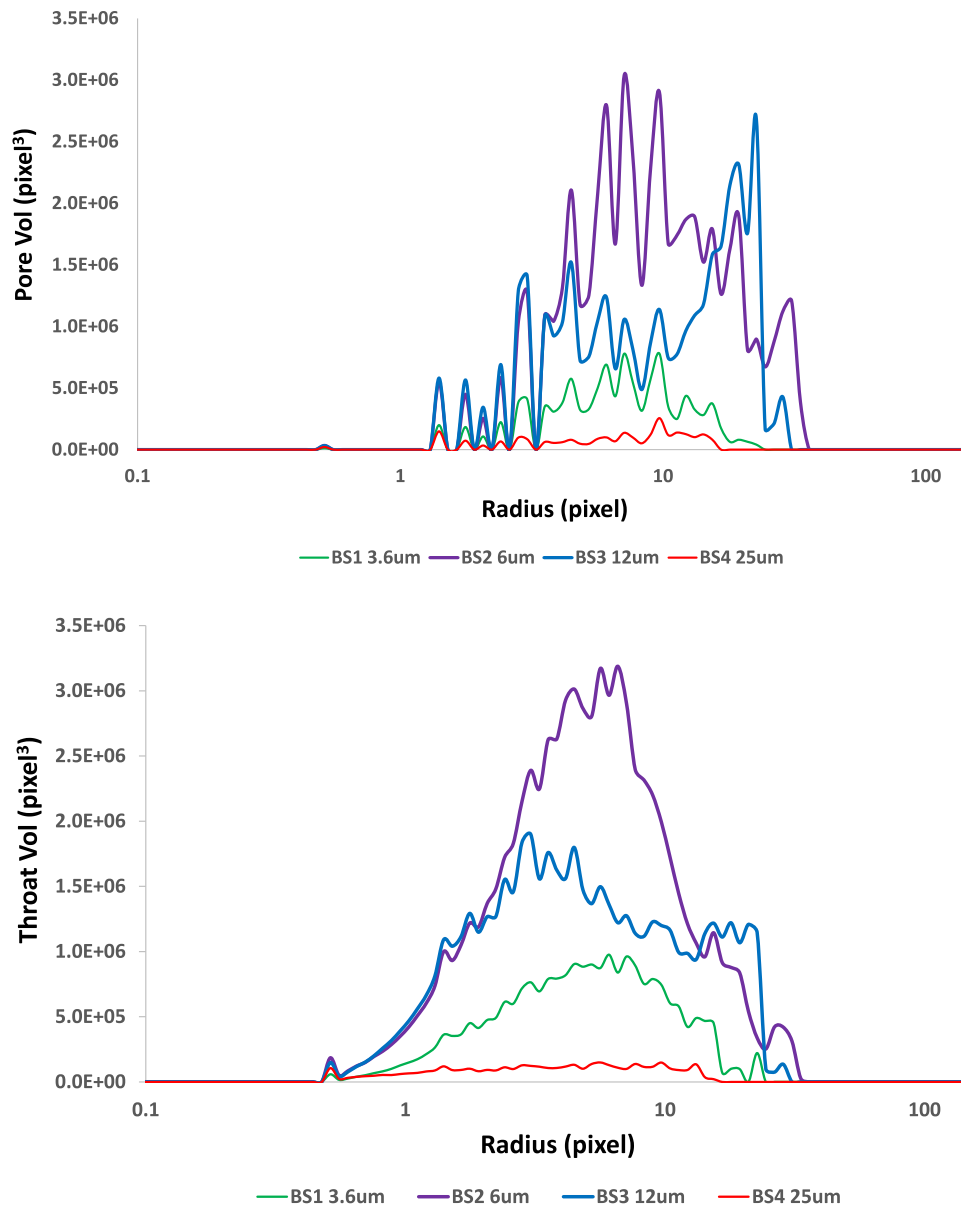


FIGURE 6 Pore body (top) and pore throat (bottom) volumes versus radius for the four samples.

more than one network is based on the original data from the skeletons (pore bodies and throats), as described using the stochastic approach from PoreStudio. The PNM extracted from the higher resolution μ CT volume (the finer network) is hence combined with a coarser network.

A specific objective of our study was to apply an REV analysis of the hydraulic conductivity of the largest soil sample (BS4) imaged at the lower resolution. We wanted to know which one of the smaller digital BS1, BS2, or BS3 could best enhance the pore network of the larger sample. The REV is used here to define the fundamental size for the hydraulic conductivity measurements, those of the simulations, and their respective averages (i.e., x_{mean}). We further used the coefficient of variation (C_v) as a dimensionless measure of the heterogeneity of a sample. As reported by Vik et al. (2013),

C_v is defined as the ratio between the standard deviation of a property and the property arithmetic mean:

$$C_v = \frac{\sqrt{\text{Var}(x)}}{x_{\text{mean}}} \left[1 + \frac{1}{4(n-1)} \right] \quad (4)$$

in which the second part of the equation is a correction when the number of samples (n) is equal to or <10 . The hydraulic conductivity class is based on the C_v value, and the sample is considered homogeneous when C_v is <0.5 . In our study, the C_v was evaluated to be 0.28.

The pore network flow simulations were carried out for all sub-samples. For the REV study, we used modules in the PoreStudio software to digitally divide the coarser pore network of sample BS4 into 10 pieces and then estimated

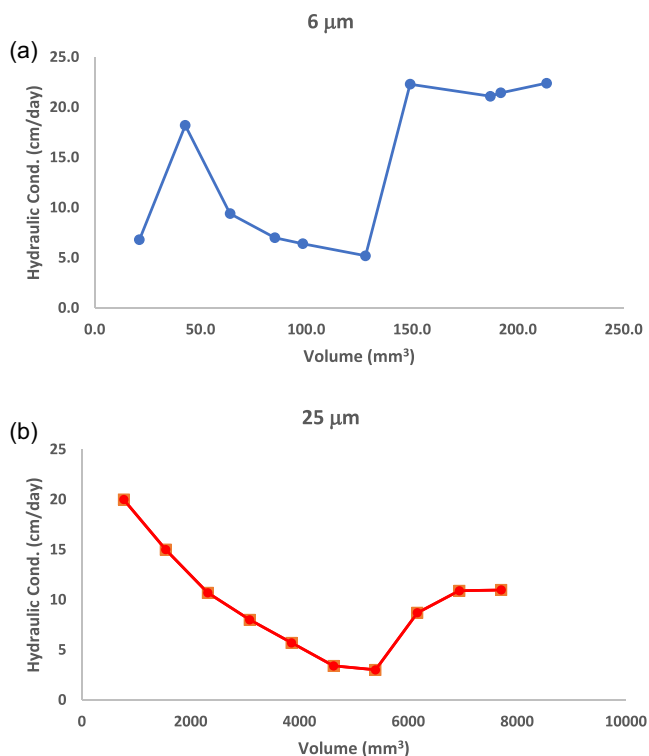


FIGURE 7 Evaluation of hydraulic conductivity by volume: (a) BS2 (6 μm) and (b) BS4 (25 μm).

the porosity and saturated hydraulic conductivity (K_s) of an increasingly larger set of combined subsamples until the porosity or conductivity stabilized. For the porosity, the REV could be easily determined. However, the results in Figure 7 indicate that sample BS4 could not reach a constant plateau, except for the last two points. This means that the REV for K_s could not be defined well due to soil heterogeneity, and hence that the REV size for the proposed methodology should be about 7000 mm³ or larger (Zhang et al., 2022).

Following Jiang et al. (2012) and others, the geometry and topology of the individual networks were described statistically in terms of probability distributions of the volume, radius, and connectivity of the network elements. The next step was to generate stochastic digital samples based on the original skeletons (Raouf & Hassanzadeh, 2010; Raouf et al., 2013). For this purpose, we used PoreStudio to generate a stochastic sample of BS4, as well as of the other samples, based on their original average connectivity and the original sets of pore body and pore throat radii. The placement of pore bodies and throats in the network was made stochastically by the program.

The best distributions for the networks were found to be lognormal. Figure 8 shows the histogram of the BS4 throat length and the fitted lognormal distribution.

Using the pore network generation module of PoreStudio (2023), the stochastic BS4 sample was generated assuming the same average connectivity of the original and stochastic

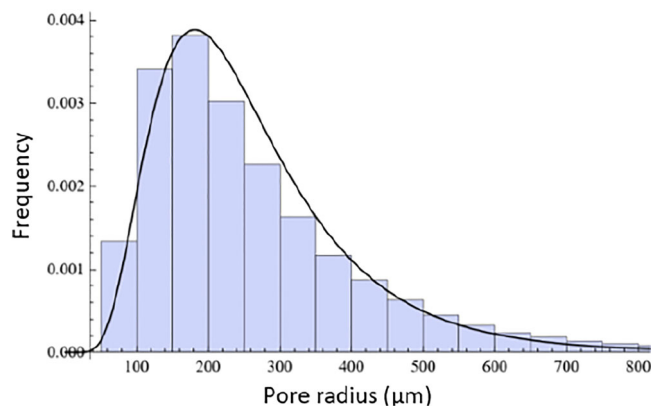


FIGURE 8 Histogram of the pore throat radius of sample BS4.

skeletons. This is done by statistically placing the pore bodies and pore throats in the new skeleton. We verified results obtained with the stochastic sample of BS4 with the original digital sample. Figure 9a compares pore throat volumes (by radius) obtained using PoreStudio with those obtained with the software for the stochastic sample (along with the sample correlations), while results for the pore body volumes are shown in Figure 9b. The pore connectivity had a variation of 6% comparing the stochastic with the original digital sample. The data show good agreement, including the generated curves. Table 3 provides an overview of all BS4 pore network modeling results.

To capture the multiscale PSD of the rock, we imaged four different soil samples at different resolutions and integrated the data to produce a pore-network model that combines information at several length scales that cannot be recovered from a single tomographic image. We used the network integration approach of Jiang et al. (2007, 2013) to generate PNMs of arbitrarily large volumes that can incorporate multiscale pore systems extracted from images obtained at different resolutions. The larger volume sample in our study was BS4, imaged with a resolution of 25 μm, in which we then incorporated features extracted from the other systems (3.6, 6, and 12 μm scans). Sample BS4 showed less pores and throats, compared with the other samples, and also had a lower hydraulic conductivity. The conductivity, connectivity, and total porosity all showed increasing trends with the imaging resolution. Sample BS1 had the finest network and displayed a calculated hydraulic conductivity value higher than the values estimated from the particle size distribution and approximate field estimates.

We explored three different combinations of samples to generate the scaled stochastic samples, that is, by combining BS4 and BS1, BS4, and BS2, and BS4 + BS3. In all cases, we used BS4 since this sample had the largest (and coarsest) network with the largest pores and combined its network with those of the smaller sample with higher resolution to better capture the smaller pore bodies and pore

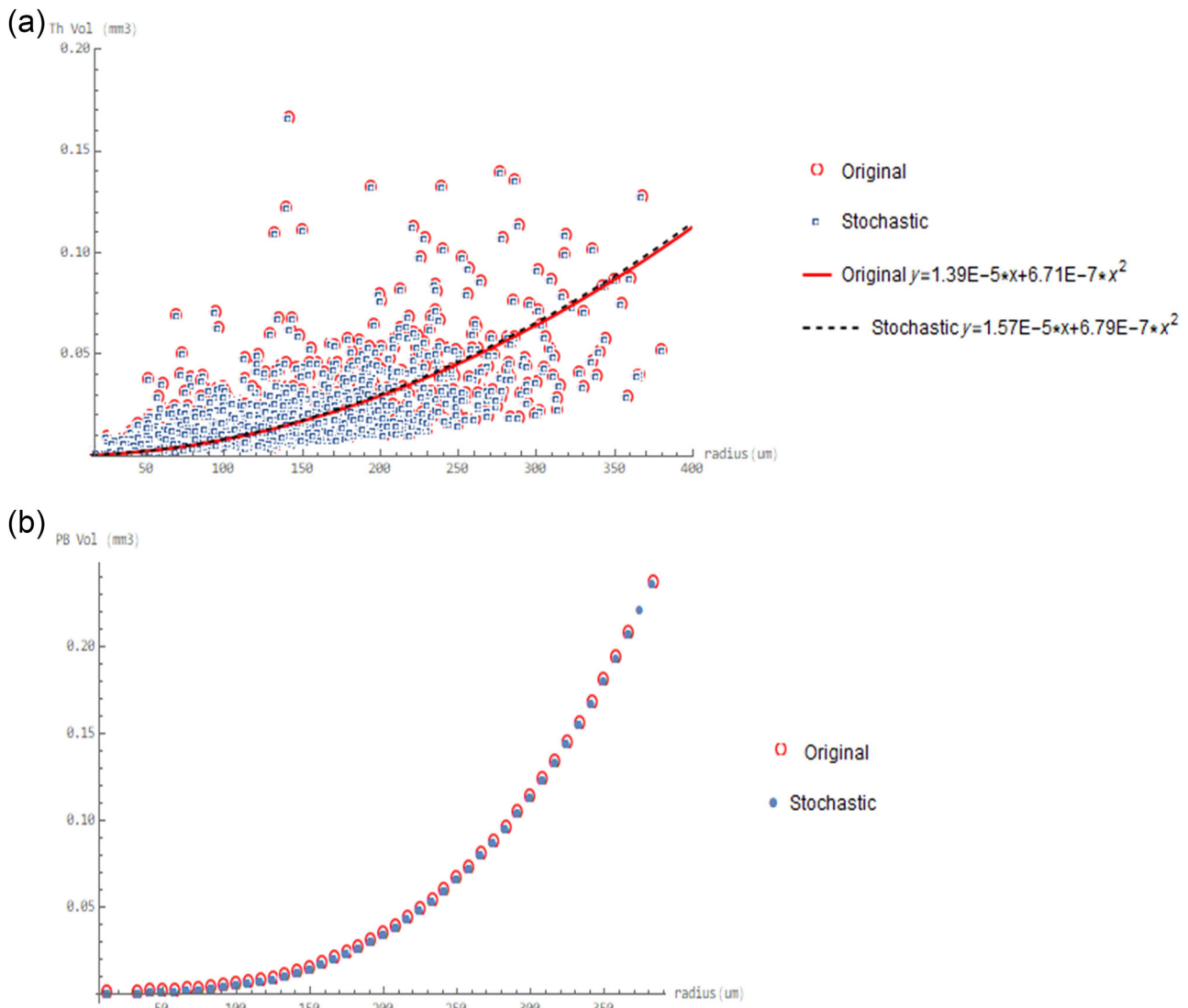


FIGURE 9 Correlation of the digital and stochastic pore throat (a) and pore body (b) volumes of sample BS4.

TABLE 3 Pore network model (PNM) parameters and results.

Samples	Throats	Pore bodies	Volume (mm ³)	Porosity	Conductivity (cm/day)
BS4 original	65,844	60,476	7711.3	0.135	10.96
BS4 stochastic	66,736	61,447	7732.0	0.132	10.80

throats. Combining the pore systems of two networks facilitated having enough overlap to include the representation of intermediate-size pores.

PNM results obtained with the combinations of 25 + 3.6 μm, 25 + 6 μm, and 25 + 12 μm are reported in Table 4. The best results were obtained by combining the μCT images with resolutions of 6 μm (BS2) and 25 μm (BS4). The PNM modeled hydraulic conductivity of sample BS2 imaged at a resolution of 6 μm was closest to the estimated value of 24.7 cm/day. The pore system of sample BS4 received the

finer part of the BS2 network and hence also had a higher K_s value. The combination of BS4 and BS2 pore throats and pore bodies showed an increase relative to the BS4 skeleton but remained less than K_s of the BS2 skeleton. This means that the two samples had a good area of overlap in their pore systems.

The combination of BS4 and BS1 skeletons gave the second-best estimate of the hydraulic conductivity, but with the number of pore bodies and pore throats being very close to the sum of the amounts of both skeletons. This means

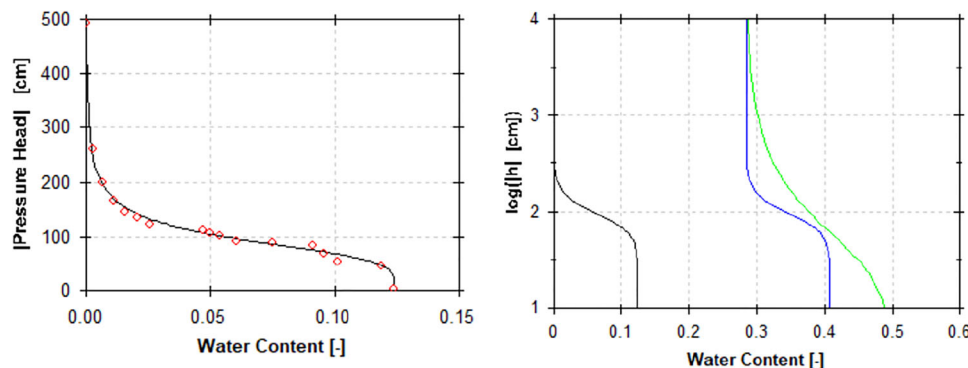


FIGURE 10 PoreStudio generated water retention data and fitted curve of the fine-textured soil (left) and comparison of the optimized PoreStudio generated retention curve (black line) with the PoreStudio curve adjusted with the residual water content (blue line) and the laboratory-measured retention curve (green line) (right).

TABLE 4 Pore networking modeling results using the combined skeletons of two samples.

Sample	Pore throats	Pore bodies	Conductivity (cm/day)
BS4 + BS1	158,021	128,549	20.1
BS4 + BS2	277,953	204,449	22.3
BS4 + BS3	120,953	100,729	18.0

that the pore systems of the two samples had a very narrow overlap range. Finally, the combination of BS4 and BS3 gave the smallest improvement in the BS4 conductivity; the skeletons of the generated pore network (pore bodies and pore throats) showed a much broader overlap in their pore systems.

Much of the above analysis focused on the saturated hydraulic conductivity, K_s , which is determined mostly by the larger connected pores. We also still ran PoreStudio for the various networks to obtain predictions of the soil water retention curve. Figure 10 shows the results for the pore network of sample BS1. The PoreStudio calculations were based on a pore network made up of mostly connected pore bodies and pore throats and do immediately account for the presence of a residual water content (θ_r), as is assumed in most standard formulations of the water retention curve. The residual water content of especially fine-textured soils can be quite large, as is the case for the selected clay soil in our study. One could correct for this reason the PoreStudio results with the residual water content of $0.284 \text{ cm}^3/\text{cm}^3$ (Figure 1). This would produce the middle curve in Figure 10, which is still about 0.08 units below the measured curve near saturation and has a higher value of the van Genuchten G_n parameter (4.66 vs. 1.75 for the laboratory-measured curve). These differences point to a need to measure water contents in the very dry range, including portions of the curve where corner, film, and vapor flow become important (e.g., Peters et al., 2015).

This issue appears is important for fine-textured (clay) soils, such as those used in this study, since their nano-size pores are below the resolution of most or all μCT methods (e.g., Godoy et al., 2024).

4 | CONCLUSIONS

In this study, we showed one way of combining the μCT results obtained for samples having different sizes and imaged with different resolutions, with as ultimate objective to obtain more representative conductivity/permeability estimate of the larger sample imaged with a lower resolution. The idea is to obtain simpler pore networks, based on μCT stacks of the soil or rock samples, that carry information from distinct samples imaged at higher resolutions and is implemented in pore networks obtained from lower resolution imaging. The technique provides samples with a less-refined pore system that if scanned at very high resolution, thus permitting one to perform other modeling studies such as contaminant transport and multiphase flow in less time and with less computational demands. The procedure was illustrated here by combining the images of two skeletons obtained with different resolutions. The approach can be extended to more than two samples by using the same steps as described in this paper.

AUTHOR CONTRIBUTIONS

Elizabeth M. Pontedeiro: Conceptualization; methodology; writing—original draft. **Martinus Th. van Genuchten:** Supervision; writing—review and editing. **William Godoy:** Formal analysis; software. **Mateus G. Ramirez:** Conceptualization; formal analysis. **Carlos M. P. Vaz:** Data curation; writing—review and editing. **Silvio Crestana:** Supervision; writing—review and editing. **Maira C. O. Lima:** Writing—review and editing. **Paulo Couto:** Supervision. **Jian Su:** Supervision; writing—review and editing.

CONFLICT OF INTEREST STATEMENT


The authors declare no conflicts of interest.

ORCID

Elizabeth M. Pontedeiro  <https://orcid.org/0000-0003-1418-3314>

Martinus Th. van Genuchten  <https://orcid.org/0000-0003-1654-8858>

William Godoy  <https://orcid.org/0000-0003-1879-9386>

Mateus G. Ramirez  <https://orcid.org/0000-0002-2268-3274>

Carlos M. P. Vaz  <https://orcid.org/0000-0003-1336-8958>

Paulo Couto  <https://orcid.org/0000-0002-3847-8638>

REFERENCES

- Allaire, S. E., Roulier, S., & Cessna, A. J. (2009). Quantifying preferential flow in soils: A re-view of different techniques. *Journal of Hydrology*, *378*, 179–204. <https://doi.org/10.1016/j.jhydrol.2009.08.013>
- Blunt, M. J., Bijeljic, B., Dong, H., Gharbi, O., Iglauer, S., Mostaghimi, P., Paluszny, A., & Pentland, C. (2013). Pore-scale imaging and modelling. *Advances in Water Resources*, *51*, 197–216. <https://doi.org/10.1016/j.advwatres.2012.03.003>
- Cássaro, F. A. M., Durand, A. N. P., Gimenez, D., & Vaz, C. M. P. (2017). Pore size distributions of soils derived using a geometrical approach and multiple resolution microCT images. *Soil Science Society of America Journal*, *81*, 468–476. <https://doi.org/10.2136/sssaj2016.09.0291>
- Cnudde, V., & Boone, M. N. (2013). High-resolution X-ray computed tomography in geosciences: A review of the current technology and applications. *Earth-Sciences Review*, *123*, 1–17. <http://doi.org/10.1016/j.earscirev.2013.04.003>
- Crestana, S., & Cruvinel, P. E. (2023). Developing spectroscopic and imaging techniques for advanced studies in soil physics based on results obtained at Embrapa instrumentation. *Brazilian Journal of Physics*, *52*(6), Article 200. <https://doi.org/10.1007/s13538-022-01202-8>
- Dragonfly. (2022). *Dragonfly 2022.2* [Computer software]. Comet Technologies Canada Inc. <https://www.theobjects.com/dragonfly>
- Elahmani, A., Al-Raoush, R. I., Abugazia, H., & Seers, T. (2022). Pore-scale simulation of fine particles migration in porous media using coupled CFD-DEM. *Powder Technology*, *398*, 117130. <https://doi.org/10.1016/j.powtec.2022.117130>
- Godoy, W., Pontedeiro, E. M., Barros, R. A. B. R., de Vries, E. T., Raoof, A., van Genuchten, M. Th., & Couto, P. (2024). Modeling sub-resolution porosity of a heterogeneous carbonate rock sample. *Vadose Zone Journal*. <https://doi.org/10.1002/vzj2.20348>
- Godoy, W., Pontedeiro, E. M., Hoerlle, F., Raoof, A., van Genuchten, M. Th., Santiago, J., & Couto, P. (2019). Computational and experimental pore-scale studies of a carbonate rock sample. *Journal of Hydrology and Hydromechanics*, *67*(4), 372–383. <https://doi.org/10.2478/johh-2019-0009>
- Hebert, V., Garing, C., Luquot, L., Pezard, P. A., & Gouze, P. (2014). Multi-scale X-ray tomography analysis of carbonate porosity. In S. M. Agar & S. Geiger (Eds.), *Fundamental controls on fluid flow in carbonates: Current workflows to emerging technologies* (Vol. 406, 61–79). Geological Society Special Publication.
- Jiang, Z., van Dijke, M., Sorbie, K., & Couples, G. (2013). Representation of multiscale heterogeneity via multiscale pore networks. *Water Resources Research*, *49*, 5437–5449. <https://doi.org/10.1002/wrcr.20304>
- Jiang, Z., van Dijke, M., Wu, K., Couples, G., Sorbie, K., & Ma, J. (2012). Stochastic pore network generation from 3D rock images. *Transport in Porous Media*, *94*, 571–593. <https://doi.org/10.1007/s11242-011-9792-z>
- Jiang, Z., Wu, K., Couples, G., van Dijke, M., Sorbie, K., & Ma, J. (2007). Efficient extraction of networks from three-dimensional porous media. *Water Resources Research*, *43*, W12S03. <https://doi.org/10.1029/2006WR005780>
- Kastner, J., Zaunschirm, S., Rendl, S., & da Silva, E. P. (2021). Influence of rheocasting and rare earth metals on the 3D-microstructure of ZK60 Mg-alloy measured by multiscale X-ray computed tomography. *Materials Characterization*, *174*, 110996. <https://doi.org/10.1016/j.matchar.2021.110996>
- Katuwal, S., Hermansen, C., Knadel, M., Moldrup, P., Greve, M. H., & de Jonge, L. W. (2018). Combining X-ray computed tomography and visible near-infrared spectroscopy for prediction of soil structural properties. *Vadose Zone Journal*, *17*, 160054. <https://doi.org/10.2136/vzj2016.06.0054>
- Lima, M. C. O., Pontedeiro, E. M., Ramirez, M. G., Favoreto, J., Santos, H. N., van Genuchten, M. Th., Borghi, L., Couto, P., & Raoof, A. (2022). Impacts of mineralogy on petrophysical properties. *Transport in Porous Media*, *145*, 103–125. <https://doi.org/10.1007/s11242-022-01829-w>
- Lima, M. C. O., Pontedeiro, E. M. B. D., Ramirez, M. G., Boyd, A., van Genuchten, M. Th., Borghi, L., Couto, P., & Raoof, A. (2020). Petrophysical correlations for permeability of coquinas (carbonate rocks). *Transport in Porous Media*, *135*, 287–308. <https://doi.org/10.1007/s11242-020-01474-1>
- Mehmani, A., Kelly, S., & Torres-Verdín, C. (2020). Leveraging digital rock physics workflows in unconventional petrophysics: A review of opportunities, challenges, and benchmarking. *Journal of Petroleum Science and Engineering*, *190*, 107083. <https://doi.org/10.1016/j.petrol.2020.107083>
- Menke, H. P., Andrew, M. G., Blunt, M. J., & Bijeljic, B. (2016). Reservoir condition imaging of reactive transport in heterogeneous carbonates using fast synchrotron tomography; Effect of initial pore structure and flow conditions. *Chemical Geology*, *428*, 15–26. <https://doi.org/10.1016/j.chemgeo.2016.02.030>
- Pak, T., Butler, I. B., Geiger, S., van Dijke, M. I. J., Jiang, Z., & Surmas, R. (2016). Multiscale pore network representation of heterogeneous carbonate rocks. *Water Resources Research*, *52*, 5433–5441. <https://doi.org/10.1002/2016WR018719>
- Peters, A., Iden, S. C., & Durner, W. (2015). Revisiting the simplified evaporation method: Identification of hydraulic functions considering vapor, film and corner flow. *Journal of Hydrology*, *527*, 531–542. <https://doi.org/10.1016/j.jhydrol.2015.05.020>
- Piccoli, I., Schjønning, P., Lamandé, M., Zaninid, F., & Moraria, F. (2019). Coupling gas transport measurements and X-ray tomography scans for multiscale analysis in silty soils. *Geoderma*, *338*, 576–584. <https://doi.org/10.1016/j.geoderma.2018.09.029>
- PoreStudio. (2023). *PoreStudio*. <https://porestudio.com>
- Raoof, A., & Hassanizadeh, S. M. (2010). A new method for generating pore-network models of porous media. *Transport in Porous Media*, *81*(3), 391–407. <https://doi.org/10.1007/s11242-009-9412-3>

- Raouf, A., Nick, H. M., Hassanizadeh, S. M., & Spiers, C. J. (2013). PoreFlow: A complex pore-network model for simulation of reactive transport in variably saturated porous media. *Computers & Geosciences*, *61*, 160–174. <https://doi.org/10.1016/j.cageo.2013.08.005>
- Ruspini, L. C., Øren, P. E., Berg, S., Masalmeh, S., Bultreys, T., Taberner, C., Sorop, T., Marcelis, F., Appel, M., Freeman, J., & Wilson, O. B. (2021). Multiscale digital rock analysis for complex rocks. *Transport in Porous Media*, *139*, 301–325. <https://doi.org/10.1007/s11242-021-01667-2>
- Sadeghnejad, S., & Gostick, J. (2020). Multiscale reconstruction of vuggy carbonates by pore-network modeling and image-based technique. *SPE Journal*, *25*(01), 253–267. <https://doi.org/10.2118/198902-PA>
- Salek, M. F., & Beckingham, L. E. (2023). Effect of X-ray computed tomography imaging parameters on quantification of petrophysical properties. *Earth and Space Science*, *10*, e2023EA003095. <https://doi.org/10.1029/2023EA003095>
- Schaap, M. G., Leij, F. J., & van Genuchten, M. Th. (2001). Rosetta: A computer program for estimating soil hydraulic parameters with hierarchical pedotransfer functions. *Journal of Hydrology*, *251*(3–4), 163–176. [https://doi.org/10.1016/S0022-1694\(01\)00466-8](https://doi.org/10.1016/S0022-1694(01)00466-8)
- Silveira, T. M., Hoerle, F., Rocha, A. S., Lima, M. C. O., Ramirez, M. G., Pontedeiro, E. M., Genuchten, M., Cruz, D. O. A., & Couto, P. (2022). Effects of carbonated water injection on the pore system of a carbonate rock (coquina). *Journal of Hydrology and Hydromechanics*, *70*(2), 1–12. <https://doi.org/10.2478/johh-2022-0001>
- Thermo Fisher Scientific. (2022). *Avizo* (Version 2022.2) [Computer software]. <https://www.fei.com/software/amira-avizo/>
- van Genuchten, M. Th. (1980). A closed form equation for predicting the hydraulic conductivity of unsaturated soils. *Soil Science Society of America Journal*, *44*, 892–898. <https://doi.org/10.2136/sssaj1980.036159950044000500002x>
- Van Offenwert, S., Cnudde, V., & Bultreys, T. (2019). Pore-scale visualization and quantification of transient solute transport using fast microcomputed tomography. *Water Resources Research*, *55*(11), 9279–9291. <https://doi.org/10.1029/2019WR025880>
- Vaz, C. M. P., de Maria, I. C., Lasso, P. O., & Tuller, M. (2011). Evaluation of an advanced benchtop micro-computed tomography system for quantifying porosities and pore-size distributions of two Brazilian oxisols. *Soil Science Society of America Journal*, *75*(3), 832–841. <https://doi.org/10.2136/sssaj2010.0245>
- Vaz, C. M. P., Tuller, M., Lasso, P. R. O., & Crestana, S. (2014). New perspectives for the application of high-resolution benchtop X-ray MicroCT for quantifying void, solid and liquid phases in soils. In W. G. Teixeira, M. B. Ceddia, M. V. Ottoni, & G. K. Donnagema (Eds.), *Application of soil physics in environmental analyses: Measuring, modelling and data integration, progress in soil science* (pp. 261–281). Springer. https://doi.org/10.1007/978-3-319-06013-2_12
- Verri, I., Torre, A. D., Montenegro, G., Onorati, A., Duca, S., Mora, C. A., Radaelli, F., & Trombin, G. (2017). Development of a digital rock physics workflow for the analysis of sandstones and tight rocks. *Journal of Petroleum Science and Engineering*, *156*, 790–800. <https://doi.org/10.1016/j.petrol.2017.06.053>
- Vik, B., Bastesen, E., & Skauge, A. (2013). Evaluation of representative elementary volume for a vuggy carbonate rock, Part 1: Porosity, permeability and dispersivity. *Journal of Petroleum Science and Engineering*, *112*, 36–47. <https://doi.org/10.1016/j.petrol.2013.03.029>
- Wildenschild, D., & Sheppard, A. P. (2013). X-ray imaging and analysis techniques for quantifying pore-scale structure and processes in sub-surface porous medium systems. *Advances in Water Resources*, *51*, 217–246. <https://doi.org/10.1016/j.advwatres.2012.07.018>
- Wu, K., Jiang, Z., Ma, J., Couples, G. D., van Dijke, M. I. J., & Sorbie, K. S. (2011). *Multiscale pore system reconstruction and integration*. International Symposium Society of Core Analysts.
- Xiong, Q., Baychev, T. J., & Jivkov, A. P. (2016). Review of pore network modelling of porous media: Experimental characterisations, network constructions and applications to reactive transport. *Journal of Contaminant Hydrology*, *192*, 101–117. <http://dx.doi.org/10.1016/j.jconhyd.2016.07.002>
- Yang, Z., Peng, X.-F., Lee, D.-J., & Chen, M.-Y. (2009). An image-based method for obtaining pore-size distribution of porous media. *Environmental Science & Technology*, *43*(9), 3248–3253. <https://doi.org/10.1021/es900097e>
- Yao, J., Liu, L., Yang, Y., Sun, H., & Zhang, L. (2023). Characterizing multi-scale shale pore structure based on multi-experimental imaging and machine learning. *Natural Gas Industry*, *10*, 361–371. <https://doi.org/10.1016/j.ngib.2023.07.005>
- Zhang, H., Abderrahmane, H. A., Arif, M., Kobaisi, M., & Sassi, M. (2022). Influence of heterogeneity on carbonate permeability upscaling: A renormalization approach coupled with the pore network model. *Energy Fuels*, *36*, 3003–3015. <https://doi.org/10.1021/acs.energyfuels.1c04010>
- Zubeldia, E. H., Ozelim, L. C. de S. M., Cavalcante, A. L. B., & Crestana, S. (2016). Cellular automata and x-Ray microcomputed tomography images for generating artificial porous media. *International Journal of Geomechanics*, *16*(2), 04015057. [https://doi.org/10.1061/\(ASCE\)GM.1943-5622.0000527](https://doi.org/10.1061/(ASCE)GM.1943-5622.0000527)

How to cite this article: Pontedeiro, E. M., van Genuchten, M. Th., Godoy, W., Ramirez, M. G., Vaz, C. M. P., Crestana, S., Lima, M. C. O., Couto, P., & Su, J. (2024). Multiscale pore-network reconstruction of a fine-textured heterogeneous soil. *Vadose Zone Journal*, e20354. <https://doi.org/10.1002/vzj2.20354>